AD-A159 806 INVERSE FARADAY EFFECT IN HEMOGLOBIN DETECTED BY RAMAN SPECTROSCOPY: AN E.. (U) NAVAL AIR SYSTEMS COMMAND WASHINGTON DC T W BARRETT 03 JUN 85 NADC-85074-60 1/1

UNCLASSIFIED F/G 6/1 NL

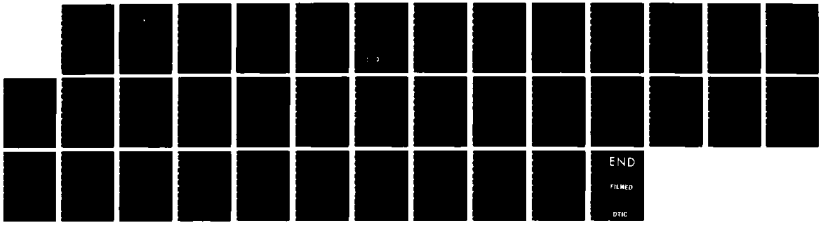

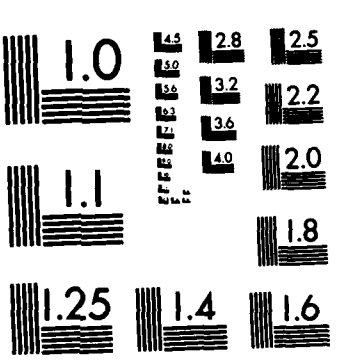

(12)

REPORT NO. NADC-85074-60

AD-A159 806

INVERSE FARADAY EFFECT IN HEMOGLOBIN DETECTED BY RAMAN SPECTROSCOPY: AN EXAMPLE OF MAGNETIC RESONANCE RAMAN ACTIVITY

T. W. Barrett
NAVAL AIR SYSTEMS COMMAND
Department of the Navy
Washington, DC 20361

3 JUNE 1985

FINAL REPORT

Approved for Public Release; Distribution Unlimited

Prepared for
NAVAL AIR DEVELOPMENT CENTER
Warminster, Pennsylvania 18974-5000

NOTICES

REPORT NUMBERING SYSTEM – The numbering of technical project reports issued by the Naval Air Development Center is arranged for specific identification purposes. Each number consists of the Center acronym, the calendar year in which the number was assigned, the sequence number of the report within the specific calendar year, and the official 2-digit correspondence code of the Command Office or the Functional Directorate responsible for the report. For example: Report No. NADC-78015-20 indicates the fifteenth Center report for the year 1978, and prepared by the Systems Directorate. The numerical codes are as follows:

CODE	OFFICE OR DIRECTORATE
00	Commander, Naval Air Development Center
01	Technical Director, Naval Air Development Center
02	Comptroller
10	Directorate Command Projects
20	Systems Directorate
30	Sensors & Avionics Technology Directorate
40	Communication & Navigation Technology Directorate
50	Software Computer Directorate
60	Aircraft & Crew Systems Technology Directorate
70	Planning Assessment Resources
80	Engineering Support Group

PRODUCT ENDORSEMENT – The discussion or instructions concerning commercial products herein do not constitute an endorsement by the Government nor do they convey or imply the license or right to use such products.

UNCLASSIFIED
SECURITY CLASSIFICATION OF THIS PAGE

AD-A159 806

REPORT DOCUMENTATION PAGE

1a REPORT SECURITY CLASSIFICATION: Unclassified	1b RESTRICTIVE MARKINGS: N/A
2a SECURITY CLASSIFICATION AUTHORITY: N/A	3 DISTRIBUTION/AVAILABILITY OF REPORT: Approved for Public Release; Distribution Unlimited
2b DECLASSIFICATION/DOWNGRADING SCHEDULE: N/A	
4 PERFORMING ORGANIZATION REPORT NUMBER(S): N/A	5 MONITORING ORGANIZATION REPORT NUMBER(S): NADC-85074-60
6a NAME OF PERFORMING ORGANIZATION: Naval Air Systems Command; 6b OFFICE SYMBOL (If applicable): 310P	7a NAME OF MONITORING ORGANIZATION: Aircraft and Crew Systems Technology Directorate
6c ADDRESS (City, State, and ZIP Code): Department of the Navy, Washington, DC 20361	7b ADDRESS (City, State, and ZIP Code): Naval Air Development Center, Warminster, PA 18974
8a NAME OF FUNDING/SPONSORING ORGANIZATION: Naval Air Development Center; 8b OFFICE SYMBOL (If applicable): 6062	9 PROCUREMENT INSTRUMENT IDENTIFICATION NUMBER: N/A
8c ADDRESS (City, State, and ZIP Code): Warminster, PA 18974	10 SOURCE OF FUNDING NUMBERS: PROGRAM ELEMENT NO: N/A; PROJECT NO: N/A; TASK NO: N/A; WORK UNIT ACCESSION NO: N/A

11 TITLE (Include Security Classification)
Inverse Faraday Effect in Hemoglobin Detected By Raman Spectroscopy: An Example of Magnetic Resonance Raman Activity

12 PERSONAL AUTHOR(S): T. W. Barrett

13a TYPE OF REPORT	13b TIME COVERED	14 DATE OF REPORT (Year, Month, Day)	15 PAGE COUNT
Final	FROM _____ TO _____	1985 June 3	27

16 SUPPLEMENTARY NOTATION

17 COSATI CODES			18 SUBJECT TERMS (Continue on reverse if necessary and identify by block number)
FIELD	GROUP	SUB-GROUP	Hemoglobin; Porphyrin; Magnetic Resonance; Resonance Raman Light Scattering; Polarization Measurement

19 ABSTRACT (Continue on reverse if necessary and identify by block number)

A complete polarization study of human oxy- and carbonmonoxyhemoglobin A and S is reported for backscattered light in the resonance Raman light scattering situation with excitations in the long wavelength region, $\lambda = 4579$ Å and 5815 Å, and excitation in the short wavelength region, $\lambda = 4579$ Å and 4880 Å, as comparison. All four polarization components of the scattered light with respect to the two polarization conditions of linearly and circularly polarization of the incident light were measured. These were: (1) parallel; (2) perpendicular; (3) corotating; and (4) contrarotating. Keywords:

(cont.)

20 DISTRIBUTION/AVAILABILITY OF ABSTRACT	21 ABSTRACT SECURITY CLASSIFICATION
☐ UNCLASSIFIED UNLIMITED ☒ SAME AS RPT ☐ DTIC USERS	UNCLASSIFIED
22a NAME OF RESPONSIBLE INDIVIDUAL: S. R. Brown	22b TELEPHONE (Include Area Code): (215) 441-2095; 22c OFFICE SYMBOL: 6062

DD FORM 1473, 84 MAR — 83 APR edition may be used until exhausted. All other editions are obsolete.

UNCLASSIFIED

Block 19.

This method has been used to characterize the three invariants of the nonsymmetric Raman tensor for randomly oriented molecules. These invariants are based on a model in which the scattered light is dependent on only an induced electric dipole. With no higher order moments involved in the scattering process, the amplitude of any band measured under the four conditions should satisfy the relation: (1) + (2) = (3) + (4).

The experiments reported have demonstrated that although this relation is satisfied for short wavelength (4579 Å and 4880 Å) excitation, it is not satisfied for long wavelength (5682 Å and 5815 Å) excitation, for which (1) + (2) $<$ (3) + (4) holds.

The increase in light scattering is due to an inverse Faraday effect resulting in magnetic resonance Raman activity. Due to large crystal field influences and Jahn-Teller instability, the critical zero-field splitting energy is large. The incident circularly polarized radiation at $\lambda \sim 5700$ Å or $\omega \sim 17{,}544$ cm^{-1} approaches the critical cubic splitting parameter, Δ_C, the calculated value for which is 18,500 cm^{-1}. This incident light equalizes or mixes the energy levels of the $^1A_1$ and $^5T_2$ states; i.e., it populates magnetic substates. An induced electric dipole-magnetic dipole transition, besides an induced electric dipole transition, is then permitted for circularly polarized light at the Larmor precession frequency, but not permitted for linearly polarized light as the d-d metal transition is electric dipole-disallowed.

The hemoglobin S solution and gel scatters light with long wavelength excitation in a similar fashion. In addition, there are bands at 750 and 1050 cm^{-1} for the hemoglobin S gel not present in solution hemoglobin SS nor in hemoglobin A. The presence of these bands is attributed to changes in the B_{1g} mode of porphyrin ring vibrations due to the gel state.

SUMMARY

A complete polarization study of human oxy- and carbonmonoxyhemoglobin A and S is reported for backscattered light in the resonance Raman light scattering situation with excitations in the long wavelength region, λ = 4579 Å and 5815 Å, and excitation in the short wavelength region, λ = 4579 Å and 4880 Å, as comparison. All four polarization components of the scattered light with respect to the two polarization conditions of linearly and circularly polarization of the incident light were measured. These components were: (1) parallel; (2) perpendicular; (3) corotating; and (4) contrarotating.

This method has been used to characterize the three invariants of the nonsymmetric Raman tensor for randomly oriented molecules. These invariants are based on a model in which the scattered light is dependent on only an induced electric dipole. With no higher order moments involved in the scattering process, the amplitude of any band measured under the four conditions should satisfy the relation: (1) + (2) = (3) + (4).

The experiments reported have demonstrated that although this relation is satisfied for short wavelength (4579 Å and 4880 Å) excitation, it is not satisfied for long wavelength (5682 Å and 5815 Å) excitation, for which (1) + (2) < (3) + (4) holds.

The increase in light scattering is due to an inverse Faraday effect resulting in magnetic resonance Raman activity. Due to large crystal field influences and Jahn-Teller instability, the critical zero-field splitting energy is large. The incident circularly polarized radiation at $\lambda \sim 5700$ Å or $\omega \sim 17{,}544$ cm^{-1} approaches the critical cubic splitting parameter, Δ_C, the calculated value for which is 18,500 cm^{-1}. This incident light equalizes or mixes the energy levels of the $^1A_1$ and $^5T_2$ states; i.e., it populates magnetic substates. An induced electric dipole-magnetic dipole transition, besides an induced electric dipole transition, is then permitted for circularly polarized light at the Larmor precession frequency, but not permitted for linearly polarized light as the d-d metal transition is electric dipole-disallowed.

The hemoglobin S solution and gel scatters light with long wavelength excitation in a similar fashion. In addition, there are bands at 750 and 1050 cm^{-1} for the hemoglobin S gel not present in solution hemoglobin SS nor in hemoglobin A. The presence of these bands is attributed to changes in the B_{1g} mode of porphyrin ring vibrations due to the gel state.

TABLE OF CONTENTS

LIST OF TABLES

LIST OF FIGURES

INVERSE FARADAY EFFECT IN HEMOGLOBIN DETECTED BY RAMAN SPECTROSCOPY: AN EXAMPLE OF MAGNETIC RESONANCE RAMAN ACTIVITY

Terence W. Barrett
Naval Air Systems Command
Code AIR-310P
Washington, DC 20361

I. INTRODUCTION

This is a detailed report of an induced magnetic dipole moment contribution to resonance Raman scattering in hemoglobin [1]. A similar observation has been made in the case of ferrocytochrome C [2]. Such a contribution is usually very small compared with the contribution of the induced electric dipole moment [3]. However, here we report an example of magnetic resonance, whereas the off-resonance case is usually considered. The example is also unusual in that the energy, $\hbar\omega$, of the radiation in resonance with the magnetic dipole is in the visible spectrum not in the radiofrequency nor in the infrared spectrum. The resonance occurs with a zero-field splitting energy which is unusually large, due to a large crystal field influence on the iron ion of the hemoglobin chain. Δ_C, the critical cubic splitting level at which states $^1A_1$ and $^5T_2$ of the iron are equal in energy is calculated to be 18,500 cm^{-1} [4]; and the incident circularly polarized radiation at $\lambda \sim 5700$ Å or $\omega \sim 17{,}544$ cm^{-1} is of the order of this approximate calculation. This incident radiation, in resonance with zero-field split levels, acts to populate excited levels of the magnetic substates created by the crystal field. The magnetic dipole moment induced is also demonstrated to be the result of an inverse Faraday effect. We turn now from this overview of the report to the detailed theoretical basis for the experiments.

II. THEORETICAL BASIS

When either (a) the exciting radiation is near resonance with an electronic transition, or (b) in the case of electronic Raman transitions [5], or (c) in the case of transitions involving Jahn-Teller active states [6], then antisymmetric as well as symmetric components of the Raman tensor are predicted theoretically [7,8] and have been both directly measured for ferrocytochrome C [9,10], hemoglobin [11], $IrCl_6^{2-}$ [12,13], $IrBr_6^{2-}$ [14], and $FeBr_4^-$ [15].

Considering first the case of the scattered radiation due only to an induced electric dipole, the depolarization ratio has three components when there is both symmetric and antisymmetric scattering: the isotropy, $\bar{\alpha}^2$, the symmetric anisotropy, γ_s^2, and the antisymmetric anisotropy, γ_{as}^2. In order to distinguish the relative contributions of these three components to the depolarization ratio, defined:

$$\rho = \frac{I_\perp}{I_\parallel} = \frac{3\gamma_s^2 + 5\gamma_{as}^2}{45\bar{\alpha}^2 + 4\gamma_s}, \tag{1}$$

where, in terms of the elements of the Raman tensor, α_{ij}, (i = x,y,z),

$$\bar{\alpha}^2 = \frac{1}{9}(\alpha_{xx} + \alpha_{yy} + \alpha_{zz})^2, \tag{2}$$

$$\gamma_s = \frac{1}{2}[(\alpha_{xx} - \alpha_{yy})^2 + (\alpha_{yy} - \alpha_{zz})^2 + (\alpha_{zz} - \alpha_{xx})^2] + \frac{3}{4}[(\alpha_{xy} + \alpha_{yx})^2 + (\alpha_{xz} + \alpha_{zx})^2 + (\alpha_{yz} + \alpha_{zy})^2],$$

$$\gamma_{as} = \frac{3}{4}[(\alpha_{xy} - \alpha_{yx})^2 + (\alpha_{xz} - \alpha_{zx})^2 + (\alpha_{yz} - \alpha_{zy})^2],$$

at least three of the following four polarization conditions for incident and scattered light must be used in resonance Raman light scattering experiment: incident light plane polarized and the scattered light detected for the parallel polarized condition ($I_\parallel$); incident light plane polarized and scattered light detected for the perpendicularly polarized condition ($I_\perp$); incident light circularly polarized and scattered light detected for the

circularly polarized corotating condition (I_{co}); incident light circularly polarized and scattered light detected for the circularly polarized contra-rotating condition (I_{contra}).

The reversal coefficient for the scattering angle of 90° is given by:

$$R = \frac{6\gamma_s^2}{45\bar{\alpha}^2 + \gamma_s^2 + 5\gamma_{as}^2} = \frac{I_{co}}{I_{contra}} \tag{3}$$

and a general reversal coefficient dependent on the scattering angle is defined [16]:

$$R(\nu) = \frac{\frac{1-\rho}{2(1+\rho)}\sin^2\nu - \frac{1-R}{1+R}\cos\nu}{1 - \frac{1-\rho}{2(1+\rho)}\sin^2\nu + \frac{1-R}{1+R}\cos\nu} \tag{4}$$

which is a function of both ρ and R. From equations (1) and (3), it may be seen that $R(\nu)$ is a function of the three invariants, $\bar{\alpha}^2$, γ_s^2, and γ_{as}^2. Measurement of $R(\nu)$ at two different angles is thus sufficient to determine these invariants. As R(90°) = 1, but R(180°) = 1/R, the R(180°) or backscattering arrangement [17,18] must be used for the two circularly polarized conditions. The backscattering arrangement was also necessitated in the present study as concentrated solutions (gels) wre examined.

The intensities in the four polarization spectra are related to the three invariants by:

$$\begin{aligned} I_{\perp} &= 3\gamma_s^2 + 5\gamma_{as}^2, \\ I_{\parallel} &= 45\bar{\alpha}^2 + 4\gamma_s^2, \\ I_{co} &= 6\gamma_s^2, \\ I_{contra} &= 45\bar{\alpha}^2 + \gamma_s^2 + 5\gamma_{as}^2, \end{aligned} \tag{5}$$

and it is thus evident that for the case of the scattered radiation due only to an induced electric dipole:

$$I_{\perp} + I_{\parallel} = I_{co} + I_{contra}, \tag{6}$$

and only three measurements are needed, the fourth providing a check; the invariants are then related to the intensity data by:

$$6\gamma_s^2 = I_{co}, \tag{7}$$

$$5\gamma_{as}^2 = I_{\perp} - 1/2\ I_{co},$$

$$45\bar{\alpha}^2 = I_{\parallel} - 2/3\ I_{co}.$$

The McClain invariants, δ_F, δ_G, and δ_H [7,21,19,20] are related to the first set by:

$$\bar{\alpha}^2 = 1/9\ \delta_F, \tag{8}$$

$$\gamma_s^2 = 3/4\ (\delta_G + \delta_H) - 1/2\ \delta_F,$$

$$\gamma_{as}^2 = 3/4\ (\delta_G - \delta_H).$$

Both sets may be used to classify the irreducible representations of the secular point groups and thus in identifying the symmetry class of a given vibration.

So far, the scattering system has been considered as if moments higher than the induced electric dipole were not involved. This is not the case, however, with optically active molecules. A system is defined as optically active if it responds differently to right and left circularly polarized light [22,23]. The description of such optically active molecules is in terms of optically active tensors defining electric and magnetic dipoles induced by applied electric and magnetic fields, besides the polarizability tensor, which describes the relation of the induced electric dipole moment to an applied electric field.

The Hamiltonian of a system of charged particles interacting with an electromagnetic field is a multipole expansion [24] in which the semiclassical Kramers-Heisenberg dispersion equation is demonstrated to be identical with the corresponding quantum mechanical description [25]. Such a Hamiltonian, which describes a molecule in a field, is [24,26,27]:

$$\mathcal{H} = \mathcal{H}_o - d_\alpha E_\alpha - 1/3\ \Theta_{\alpha\beta} E_{\alpha\beta} - m_\alpha H_\alpha - 1/2\ \chi_{\alpha\beta} H_\alpha H_\beta, \tag{9}$$

where $\mathcal{H}_o$ is the Hamiltonian for the free molecule;

TABLE VII.
Polarized Raman intensity data for carbonmonoxyhemoglobin SS solution (arbitrary units) with 4880 Å excitation.

Band quency Δcm^{-1})	$I_{\parallel}$	$I_{\perp}$	I^*_l	I_{co}	I_{contra}	I^*_c	$I_l - I_c$	Percentage $I_c \gtrless I_l$
674	20	10	30	10	22	32	-2	7%
803	36	34	70	38	30	68	+2	5%
1371	154	35	189	55	128	183	+6	3%
1490	42	0	42	14	30	44	-2	5%
1581	55	40	95	32	65	97	-2	2%
1600	35	15	50	28	22	50	0	0%
1632	50	26	76	58	20	79	-2	3%

$I_{\parallel} + I_{\perp}$, $I_c = I_{co} + I_{contra}$

TABLE VIII.
Polarized Raman intensity data for benzene and carbontetrachloride for backscattered light.

Band quency Δcm^{-1})	$I_{\parallel}$	$I_{\perp}$	I^*_l	I_{co}	I_{contra}	I^*_c	$I_l - I_c$	Percentage $I_c > I_l$
				λ = 5145 Å, C_6H_6				
606	258	199	457	376	81	457	0	0%
				λ = 5815 Å, C_6H_6				
986	3640	136	3776	262	3400	3712	+64	0.4%
				λ = 4880 Å, CCl_4				
215	21.2	11.6	37.9	31.2	7.2	38.4	+0.6	2%
310	24.8	18.1	42.9	36.2	6.8	43.0	+0.1	0%
460	74.4	1.0	75.4	34.8	79.4	80.8	+5.4	7%
				λ = 5815 Å, CCl_4				
215	1136	828	1964	1536	339	1875	+89	4.5%
310	1216	879	2095	1700	344	2044	+51	2.4%
460	3188	166	3304	304	3192	3496	-308	5.4%

$I_{\parallel} + I_{\perp}$, $I_c = I_{co} + I_{contra}$

TABLE V.
Polarized Raman intensity data for carbonmonoxyhemoglobin AA solution (arbitrary units) with 4880 Å excitation.

Band frequency (Δcm^{-1})	$I_{\parallel}$	$I_{\perp}$	I^*_l	I_{co}	I_{contra}	I^*_c	ΣI_c	Percentage $I_c > I_l$
674	30	11	41	18	20	38	+3	7%
803	46	24	70	40	27	67	+3	4%
1371	174	34	208	48	125	173	+35	17%
1490	46	6	52	14	35	49	+3	6%
1581	60	40	100	22	62	84	+16	16%
1600	44	8	52	24	20	44	+8	15%
1632	44	28	72	49	20	69	+3	4%

*$I_l = I_{\parallel} + I_{\perp}$, $I_c = I_{co} + I_{contra}$

TABLE VI.
Polarized Raman intensity data for carbonmonoxyhemoglobin SS solution (arbitrary units) with 5815 Å excitation.

Band frequency (Δcm^{-1})	$I_{\parallel}$	$I_{\perp}$	I^*_l	I_{co}	I_{contra}	I^*_c	ΣI_c	Percentage $I_c > I_l$
677	42	6	48	8	44	52	-4	8%
748	130	95	225	175	60	235	-10	4%
974	36	30	66	64	36	100	-34	52%
993	44	29	73	60	24	84	-11	15%
1130	30	44	74	34	70	104	-31	40%
1223	90	85	175	150	49	199	-24	13%
1305	20	51	71	24	59	83	-12	17%
1342	10	55	65	44	46	90	-25	38%
1556	90	84	174	128	82	210	-36	21%
1584	122	140	162	62	138	200	-38	23%
1626	84	67	151	122	56	178	-27	18%

*$I_l = I_{\parallel} + I_{\perp}$, $I_c = I_{co} + I_{contra}$

TABLE III.

Polarized Raman intensity data for oxyhemoglobin AA (arbitrary units) with 4579 Å excitation.

Band requency (Δcm^{-1})	$I_{\parallel}$	$I_{\perp}$	I^*_{ℓ}	I_{co}	I_{contra}	I^*_c	$I_{\ell} - I_c$	Percentage $I_c > I_{\ell}$
1356	82	15	97	21	82	103	-6	6%
1474	11	4	15	3	13	16	-1	7%
1566	26	8	34	12	25	37	-3	9%
1584	13	5	18	10	9	19	-1	6%
1622	12	5	17	8	10	18	-1	6%

$I_{\ell} = I_{\parallel} + I_{\perp}$, $I_c = I_{co} + I_{contra}$

TABLE IV.

Polarized Raman intensity data for carbonmonoxyhemoglobin AA solution *(arbitrary units) with 5815 Å excitation.*

Band requency (Δcm^{-1})	$I_{\parallel}$	$I_{\perp}$	I^*_{ℓ}	I_{co}	I_{contra}	I^*_c	$I_{\ell} - I_c$	Percentage $I_c > I_{\ell}$
677	22	10	32	40	26	66	-34	106%
748	66	87	153	175	45	220	-67	43%
974	30	36	66	51	24	75	-9	14%
993	24	31	55	45	21	66	-11	20%
1130	23	46	69	18	73	91	-22	32%
1223	55	70	125	135	50	185	-60	48%
1305	5	44	49	25	50	75	-26	53%
1342	11	50	70	28	45	73	-3	4%
1556	84	62	146	140	40	180	-34	23%
1584	138	25	163	55	132	187	-24	15%
1626	80	55	135	120	58	178	-43	32%

$I_{\ell} = I_{\parallel} + I_{\perp}$, $I_c = I_{co} + I_{contra}$

TABLE I.

Polarized Raman intensity data for oxyhemoglobin AA (arbitrary units) with 5682 Å excitation.

Band frequency (Δcm^{-1})	$I_{\parallel}$	$I_{\perp}$	I^*_l	I_{co}	I_{contra}	I^*_c	$I_l - I_c$	Percentage $I_c > I_l$
604	—	19	19	30	—	30	-11	58%
676	54	—	54	46	40	86	-32	59%
756	62	51	113	45	152	197	-84	74%
1133	—	53	53	95	15	110	-57	107%
1225	50	40	90	38	104	142	-52	58%
1305	—	55	55	113	—	113	-58	105%
1342	—	80	80	123	—	123	-43	53%
1363	—	15	15	23	—	23	-8	53%
1395	—	30	30	30	—	30	0	0%
1571	45	50	95	—	110	110	-15	16%
1589	—	175	175	285	—	285	-110	63%
1638	65	42	107	30	165	195	-88	82%

*$I_l = I_{\parallel} + I_{\perp}$, $I_c = I_{co} + I_{contra}$

TABLE II

Polarized Raman intensity data for oxyhemoglobin SS gel (abitrary units) with 5682 Å excitation.

Band frequency (Δcm^{-1})	$I_{\parallel}$	$I_{\perp}$	I^*_l	I_{co}	I_{contra}	I^*_c	$I_l - I_c$	Percentage $I_c > I_l$
604	30	—	30	45	—	45	-15	50%
676	20	—	20	20	—	20	0	0%
750	37.5	56	93.5	25	94.5	119.5	-26	28%
775	50	35	85	85	40	125	-40	47%
1050	45	—	45	45	15	60	-15	33%
1133	—	48	48	35	36	71	-23	51%
1225	15	35	50	75	5	80	-30	60%
1571	25	92	117	95	58.5	153.5	-58.5	50%
1589	10	120	130	92	75	167	-37	28%
1638	35	64	99	25	115	140	-41	41%

*$I_l = I_{\parallel} + I_{\perp}$, $I_c = I_{co} + I_{contra}$

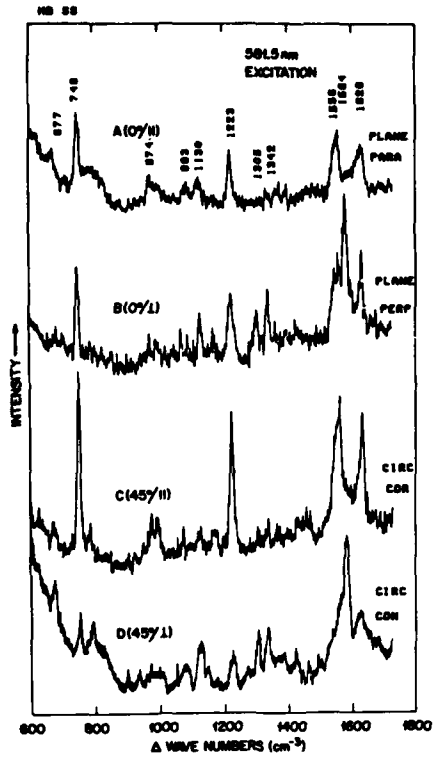

Figure 6. Resonance Raman spectra for carbonmonoxyhemoglobin S with 5815 Å excitation at 100 mW for the four polarization conditions.

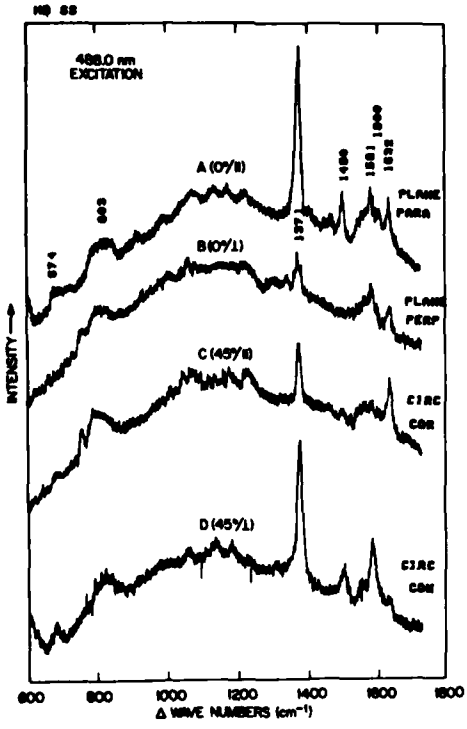

Figure 7. Resonance Raman spectra for carbonmonoxyhemoglobin S with 4880 Å excitation at 100 mW for the four polarization conditions.

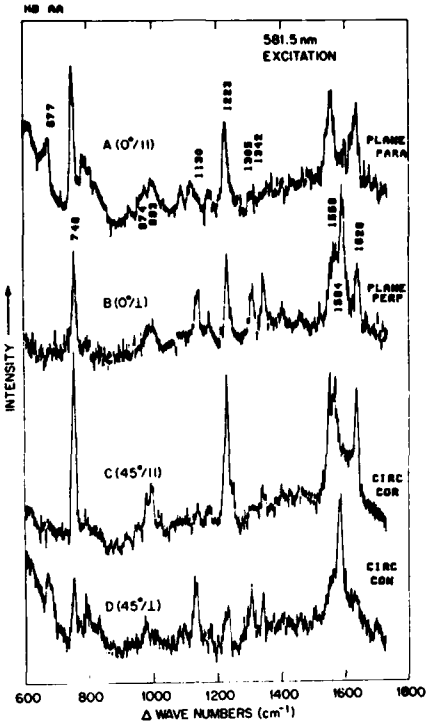

Figure 4. Resonance Raman spectra for carbonmonoxyhemoglobin A with 5815 Å excitation at 100 mW for the four polarization conditions.

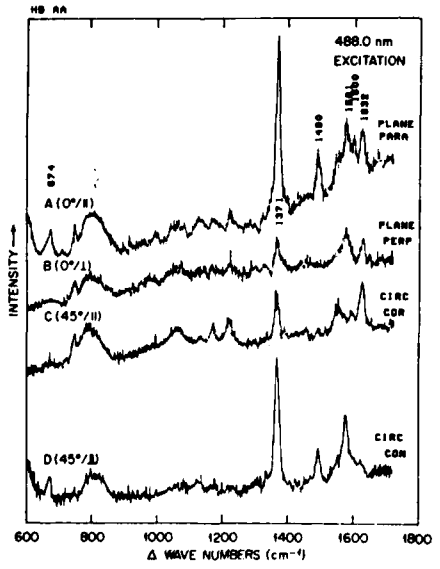

Figure 5. Resonance Raman spectra for carbonmonoxyhemoglobin A with 4880 Å excitation at 100 mW for the four polarization conditions.

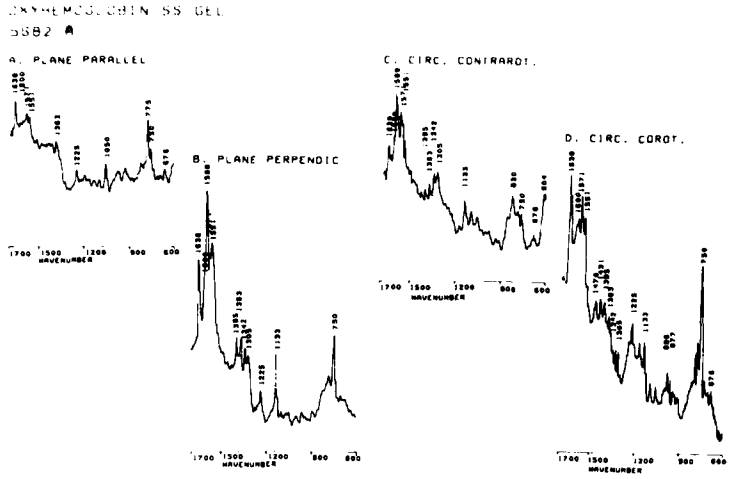

Figure 2. Resonance Raman spectra of oxyhemoglobin S gel with 5682 Å excitation at 125 mW for the four polarization conditions.

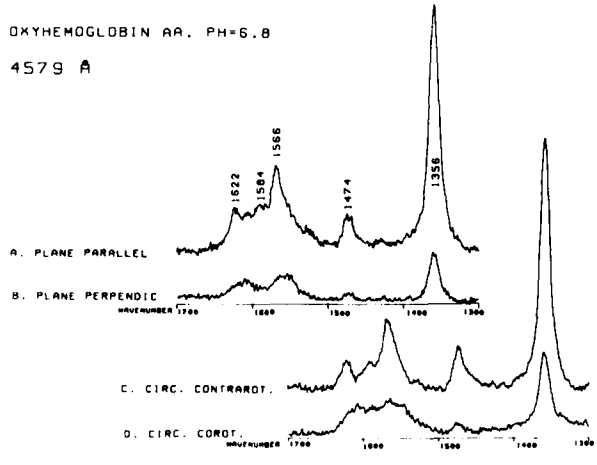

Figure 3. Resonance Raman spectra of oxyhemoglobin A with 4579 Å excitation at 100 mW for the four polarization conditions. From Ref. [1].

Figures 4-7 show the polarized spectra for carbonmonoxyhemoglobin A and S solutions with 5815 Å and 4880 Å excitation. The results of optical activity using the long wavelength (5815 Å) excitation is clearly demonstrated in Tables IV and VI, and is contrasted with the short wavelength (4880 Å) results (Tables V and VII).

Table IX lists the Raman tensor invariants for deoxyhemoglobin at 4579 Å excitation using Equ.s (7). As this interpretation is based on the validity of Equ. (6), which is rejected for 5682 Å and 5815 Å excitation, the invariants were not calculated for this excitation. The values for 1/3 (γ_s^2 - 9/4 $\bar{\alpha}^2$) are near zero for all bands, indicating an A_1 mode of the D_{4h} point group [7].

The 756 cm^{-1} depolarized line in Hb A corresponds to the 751 cm^{-1} line in nickel-octaethylporphyrin [67] and the 748 cm^{-1} line in ferrous cytochromes [68]. This line is known to show a large ($\Delta\omega$ = 67 cm^{-1}) isotropic frequency shift on deuteration in nickel-octaethylporphyrin [67] and has been assigned to the B_{1g} mode of porphyrin ring vibrations. It is therefore of some interest that this prominent band splits into two lines, one at 750, and the other at 775 cm^{-1}, in Hb S gel.

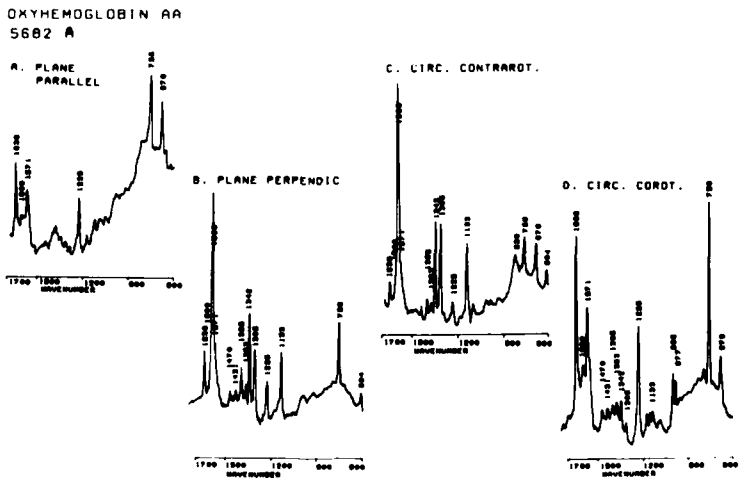

Figure 1. Resonance Raman spectra of oxyhemoglobin A with 5682 Å excitation at 100 mW for the four polarization conditions. From Ref. [1].

a JY monochromator, and amplified by the photocurrent of a cooled ITT FW 130 photomultiplier. Light was collected for 2 seconds per wavenumber.

Spectra were recorded using the 4579 Å and 4880 Å lines of a Spectra-physics 170 argon laser, the 5682 Å line of a 171 krypton laser, and the 5815 Å line of a pumped dye laser. The 5682 Å and 5815 Å excitations were in the region of the α or Q_{00} band at 5500 Å. The 4579 Å and 4880 Å excitations were in the region of the β or Q_v or Q_{01} band, which is formed at about 5000 Å by vibronic mixing between the intense, γ or B, band at about 4000 Å and the less intense Q_{00} band [64].

IV. RESULTS

The spectra obtained for both Hb A and Hb S in both the Q band and Soret band regions agree in spectral frequency with those previously reported for Q band [11] and Soret band [65] excitation.

Figures 1 and 2 show the four polarization spectra for oxyhemoglobin A and S gel in the frequency range 600–1700 cm^{-1} obtained with 5682 Å excitation. The spectra for the Hb S gel show a much reduced signal-to-noise ratio due to the diminution of coherent polarization [66]. Figure 3 shows the four polarization spectra for oxyhemoglobin A for the frequency range 1300–1700 cm^{-1} obtained with 4579 Å excitation. Tables I, II, and III list measured intensities for 5682 Å (Hb A, Table I; Hb S, Table II) and 4579 Å excitation (Hb A, Table III). In the absence of optical activity, Equ. (6) predicts that the total linearly polarized intensity, $I_\ell = I_{||} + I_{\perp}$, should be identical with the total circularly polarized intensity, $I_c = I_{co} + I_{contra}$. The differential, $I_\ell - I_c$, listed in Tables I–III therefore provides a check on the validity of the model. It is clear that the model can be rejected for 5682 Å excitation (Tables I and II), but retained for 4579 Å excitation (Table III).

geometry was requisite for these samples quite apart from the requirements of polarization sampling. Benzene and carbon tetrachloride were used as test samples for the equipment (Table VIII).

The hemoglobin A and S solutions, both oxy and carbon monoxy, other than the hemoglobin S gels, were at a concentration of 8% and in a fluid state. Although some differences between normal and sickle cell hemoglobin in the fluid state are discernible with Raman scattering [58], it is only at high concentrations that abnormalities in sickle cell hemoglobin become apparent. Some hemoglobin SS samples were therefore concentrated to a gel.

The differences between hemoglobins A and S at high concentration are explained as follows. While on the one hand, sickle cell blood has markedly decreased oxygen affinity [59], sickle cell hemoglobin in dilute solution, on the other hand, has normal functional properties, such as oxygen affinity, heme-heme interaction, Bohr effect, and reactivity with 2,3-diphosphoglycerate (2,3-DPG) and CO_2 [59-62]. However, due to the intracellular polymerization of deoxyhemoglobin S, the prediction was made that high concentrations of hemoglobin S would have low oxygen affinity. In confirmation of this prediction, May and Huehns [63] demonstrated that, while the oxygen affinity of S red cells was sharply decreased when the mean corpuscular hemoglobin concentration was increased from 10 g/100 ml, the affinity of A red cells was nearly unaffected. Thus, in order to strongly contrast the differences with normal hemoglobin, some sickle cell hemoglobin was concentrated to a gel at 24%.

The Hb A and S samples were spun at about 1000 cycles/sec in a rotating cell and the backscattered light detected, in a first series of experiments, by a Spex 1401 double monochromator, and in a second series of experiments by

components, ε_o is their mean amplitude, $\Delta\varepsilon$ is the intensity imbalance, $\Delta\bar{\nu}_{ZF}$ is the zero-field splitting, $f(\bar{\nu},\bar{\nu}_i)$ is an absorption envelope which has a peak amplitude of unity located at $\bar{\nu}_i$, and $f^{(n)}(\bar{\nu},\bar{\nu}_i)$ is the nth derivative of the shape of $f(\bar{\nu},\bar{\nu}_i)$ taken with respect to ν.

The differences between the integral and the differential techniques demonstrated by Sutherland, et al. [52,53] attributed to zero-field splitting or nondegeneracy, have been thought due to the Jahn-Teller removal of degeneracy of the porphyrin's D_{4h} symmetry to D_{2h} assisted by the crystal field potential [53], or by axial ligands with planar symmetry [54].

In summary, a major consideration of this study is, first, that a Jahn-Teller instability and a large crystal field quench angular momentum so that the zero-field energy, $E_{a_1a_2}$ of Equ. (10), is large, permitting removal of the Fe^{2+} electronic degeneracy. Then, second, (a) if the incident light is at a wavelength approximately equal to the zero-field potential energy, i.e., the light is at the Larmor precession frequency [55-57], and (b) if the incident light is circularly polarized, permitting magnetic field coupling to the metal electronic transitions, magnetic resonance occurs.

The following presents results from an examination of hemoglobin A and S solutions and hemoglobin S gels with both λ = 4579 Å, 4880 Å, 5682 Å, and 5815 Å incident light.

III. EXPERIMENTAL

The backscattering geometry used in the present study was similar to that used by Pézolet, Nafie and Peticolas [9]. Besides the theoretical justification for its use mentioned above, the backscattering geometry has the advantage that if the absorber is also the Raman scatterer, then the scattered light increases to an asymptotic limit with increasing concentration rather than going through a maximum which is characteristic of 90° geometry [17]. As some hemoglobin S samples were concentrated to a gel, the backscattering

$\underline{d}$ is taken from the multipole expansion (Atkins and Barron, 1968a):

$$H = -\underline{d}\cdot\underline{E} - \underline{m}\cdot\underline{H} + \ldots$$

and is a truncated form of Equ. (9) intepreted according to the diagrammatic perturbation theory approach of Wallace [51];

n is the number of photons; and

$E_{a_1a_2}$ is the zero field splitting energy [43].

Neglecting damping factors, a resonance occurs as $(E^2_{a_1a_2} - \hbar^2\omega^2) \rightarrow 0$, i.e., as the laser light energy approaches the negative value of the zero-field splitting energy quite independent of a resonance with electronic transitions. Thus, the calculations by Chiu [3], mentioned above, of the relative contributions of induced electric and magnetic dipole moments to normal Raman scattering do not apply in the resonance case.

The inverse Faraday effect described in Equ. (10) concerns a nonabsorbing mechanism in solutions and materials. The Raman effect is, by definition, inelastic light scattering and involves the absorption (Stokes scattering) or the annihilation (anti-Stokes scattering) of a vibronic phonon. The two are related by the induced magnetic dipole, i.e., the inverse Faraday effect results in the induction of a magnetic dipole moment by nonabsorbing mechanisms. The induced magnetic dipole then mediates increased Raman scattering for circularly polarized incident radiation at the appropriate frequency for resonance.

It is relevant to the present report that Sutherland and Klein [52] determined the absorption spectrum observed with left and right circularly polarized light for a randomly oriented solution of porphyrin molecules in the presence and absence of a magnetic field. In zero-field, the case considered in the present study, the absorption spectrum is given by:

$$\varepsilon(\bar{\nu}) = \varepsilon_0\{f(\bar{\nu},\bar{\nu}_0) + 1/2\Delta\bar{\nu}^2_{ZF}f^{(2)}(\bar{\nu},\bar{\nu}_0)\} + \Delta\varepsilon\Delta\bar{\nu}_{ZF}f^{(1)}(\bar{\nu},\bar{\nu}_0), \qquad (11)$$

where $\bar{\nu}$ is wavenumber, $\bar{\nu}_0$ is the mean position of the two unperturbed

incident light and leads to a circularly polarized component in the scattered light [40-48], one may expect an increase in Raman scattering with circularly polarized light, and Equ. (6) will not apply. Still, the amount of Raman scattering due to an induced magnetic dipole moment will generally be very much less than the amount due to an induced electric dipole moment. (Chiu [3] calculated the ratio of induced magnetic - electric dipole contributions to be $1:10^6$). Thus, the detection of a relatively large amount of Raman scattering which can be ascribed to an induced magnetic moment implicates a resonance condition. The inverse Faraday effect describes such a resonance state, to which we now turn.

The effect in which a magnetization is induced in a nonabsorbing solution or material through which is passed a polarized beam of arbitrary ellipticity is known as the inverse Faraday effect [44,49], and has been observed by Pershan et al. [49,50]. In such a situation, if $\underline{m}$ is the magnetic dipole moment operator, $\underline{k}$ is the propagation direction, and $\langle a_1|$ and $\langle a_2|$ are degenerate d electronic states split by the crystal field then [44]:

$$\langle \underline{m}\cdot\hat{\underline{k}}\rangle = \frac{2\pi n\bar{M}^2\omega^2 \sin\phi}{3V} \sum_{a_2 a_2'} \left\{ \frac{\beta C_{a_1 a_2}}{E^2_{a_1 a_2} - \bar{M}^2\omega^2} + \frac{2B^{(2)}_{a_1 a_2 a_2'}}{E_{a_1 a_2'}(E^2_{a_1 a_2} - \bar{M}^2\omega^2)} + \frac{2B^{(1)}_{a_1 a_2 a_2'}}{E_{a_2 a_2'}(E^2_{a_1 a_2} - \bar{M}^2\omega^2)} \right\}, \tag{10}$$

where $B^{(1)}_{a_1 a_2 a_2'} = \mathrm{Im}\underline{m}_{a_2 a_2'} \cdot d_{a_1 a_2'} \wedge d_{a_2 a_1}$;

$B^{(2)}_{a_1 a_2 a_2'} = \mathrm{Im}\underline{m}_{a_1 a_2'} \cdot d_{a_2 a_1} \wedge d_{a_2' a_2}$;

$C_{a_1 a_2} = \mathrm{Im}\underline{\mu}\, d_{a_1 a_2}\, d_{a_2 a_1}$; and $\wedge$ represents the average of the respective spherical tensors;

$\phi/2$ is the ellipticity of the incident light;

$\mu = \langle a_1|\underline{m}|a_1\rangle$;

V is volume;

$d_\alpha = \sum_i e_i r_i$ or the electric dipole moment;

$\Theta_{\alpha\beta} = 1/2 \sum_i e_i (3 r_{i_\alpha} r_{i_\beta} - r_i^2 \delta_{\alpha\beta})$ or the quadrupole moment,

$m_\alpha = \sum_i (e_i/2m) \varepsilon_{\alpha\beta\gamma} r_{i\beta} P_{i\gamma}$ or the magnetic moment operator for momentum $\underline{p}$;

E_α and $E_{\alpha\beta}$ are the electric field and the field gradient at the origin due to external charges;

H_α and H_β denote the magnetic field;

e_i is the ith element of charge at the point $\underline{r}_i$ relative to an origin fixed at some point on the molecule;

$\alpha\beta$ denote vector or tensor components and can be equal to x,y,z.

In the case of optically active molecules, new polarization effects arise from interference in the scattered light whose amplitude is proportional to the usual electric dipole polarizability tensor, and higher polarizability tensors [28].

In the case of molecules which are not optically active, the antisymmetric part of the real transition polarizability is generated through vibronic coupling and can only exist at absorbing frequencies. This real transition polarizability can be developed in terms of interference between an allowed electronic transition and its vibronically induced sideband, and may account for the phenomenon of inverse or anomalous polarization in hemeproteins with short wavelength excitation [11,29,30]. This explanation holds for the scattering data presented below for hemoglobin when λ = 4579 Å and 4880 Å excitation was used and when Equ. (6) is valid. This explanation also holds for spin-orbit induced antisymmetry [13,31].

However, in the case of λ = 5815 Å and 5682 Å excitation, the incident light is far removed from the Soret band absorption region [32], and is at a wavelength known to electronically absorb differentially, left versus right [33-39], i.e., to be optically active. As the intensity of Raman scattering from an optically active molecule depends on the degree of circularity of the

TABLX IX.
Ramr n tensor invariants for deoxyhemoglobin AA at 4579 Å excitation.

Band frequency (Δcm^{-1})	$9/4\bar{\alpha}^2$	$1/3\gamma_s^2$	$1/3\gamma_{as}^2$	$1/3\,(\gamma_s^2 - 9/4\,\bar{\alpha}^2)$	Classification*
1356	3.4	1.167	0.30	0.0337	A_1
1474	0.365	0.222	0.067	0.1003	A_1
1566	0.90	0.667	0.133	0.367	A_1
1584	0.32	0.556	-0.067	0.135	A_1
1622	0.333	0.444	0.067	0.333	A_1

*Contributions of (idealized) D_{4h} tensor elements to the Raman bands.

V. DISCUSSION

With long wavelength excitation, both Hb A and S demonstrate moment influences on light scattering activity higher than the induced electric dipole moment. The conditions for the validity of Equ. (6) are that the scattered light be solely dependent upon the relation between an induced electric dipole and an electric field [69]:

$$\underline{\mu} = \underline{\alpha}\,\underline{E}, \tag{12}$$

where $\underline{\mu}$ is an induced electric dipole, $\underline{\alpha}$ is the polarizability, and $\underline{E}$ is the electromagnetic field. Recent arguments concerning assymmetry of the polarizability tensor have focused on the breakdown of the Born-Oppenheimer or adiabatic approximation in the development of wave functions for the polarizability. For example, the polarizability can be separated into two parts [70]. The first, or A term, involves direct coupling of ground and resonant electronic states via the Franck-Condon overlaps. The second involves vibronic coupling of the resonant state with another excited state (B term). It has previously been thought that it is this B term, if any, which is expected to be responsible for the resonance effect [31]. Other breakdowns of the Born-Oppenheimer approximation occur when the mixing states approach one another in energy or in the excited Jahn-Teller effect, an extreme form of vibronic mixing in which the coupled states are degenerate. Yet all of these effects are handled within the framework of Equ. (12), i.e., without calling into question the nature of the Hamiltonian upon which they are based.

Given, then, not a Taylor expansion of wavefunctions, but a Taylor expansion of the electronic Hamiltonian, one is equipped to handle the inaccuracy of Equs. (6) and (12) in the case of magnetic dipole influences. Light scattering by an optically active polymer may then be characterized by invariances analogous to those of Equ. (2) but based on electric <u>and</u> magnetic dipole influences.

We turn now to consider metal-porphyrin ring and protein interactions. Shelnutt, et al. [71] have detected frequency differences up to 2 cm^{-1} in all those modes known to be sensitive to the electron density in the antibonding π^* orbitals [72]. They interpret the relationship between the frequencies of these modes and changes in the π^* orbital electron density as due to back donation from the e_g (d_π) metal orbitals to the π^* orbitals of the porphyrin macrocycle. The partial transfer of the magnetic d-electrons to the attached ions of a complex is well known [73-76]. It is relevant that the lowest unoccupied molecular orbital of the porphyrin macrocycle is the doubly degenerate, e_g (π^*) orbital [77], which is also antibonding with respect to most of the Raman-active normal modes [78]. Through back donation, the metal e_g (d_π) orbital mixes with the porphyrin π^* orbitals; and as a result, a charge is transferred from the metal orbital to the porphyrin π^* orbitals [79]. Shelnutt et al. conclude that the change in frequency of the back donation marker lines indicates that the electron densities of the porphyrin antibonding orbitals of the reduced heme are drained to about the same extent by oxygenation as they are by oxidation. As it is also these orbitals that are sensitive to the protein-heme interaction, they provide a link between oxygen bonding and the quaternary structure of proteins. ΔG, the free energy of ligand binding between the low affinity (T) and high affinity (R) quaternary structures, is postulated to contain an electronic stabilization energy resulting from a charge transfer interaction.

As a d-d metal transition is magnetic and quadrupole-allowed but electric dipole-forbidden, such a transition is permitted in the case of circularly polarized radiation, but not linearly. For resonance to occur, coupling is required to the porphyrin ring vibrations by charge transfer interactions. Charge transfer transitions are allowed by the four-orbital model of Gouterman [80,81]: namely, from the porphyrin a_{1u} and a_{2u} orbitals to the metal $d_{xz,yz}$

orbitals leading to two E_u excited states, and from the porphyrin a_{2u} orbital to the metal d_{z^2} orbital, giving rise to an A_{2u} state. The former can borrow intensity by mixing with the porphyrin α-β state, while the latter is expected to lie at higher energy and should be less intense since it cannot borrow intensity by configuration interaction [82-84]. It is significant that molecular orbital calculations which do not ignore the metal [85] result in the conclusion that the displacement of the iron atom out of the heme plane is an essential condition for a high-spin compound.

In summary, the result of the dynamic Jahn-Teller effect is a reduction in the angular momentum and the spin orbit-coupling influence of porphyrins [86,87]. This permits crystal field and spin-spin terms to dominate the zero-field splitting and the introduction of magnetic coupling between two-electron states which is spin-other-orbit controlled. In the case of zero-field splitting, there are three degenerate pairs located at z/2, 0, -z/2; and the one electron contribution to z is small, but the two-electron contribution is large. The result is that crystal field influences on zero-field splitting are large compared with internal magnetic interactions; i.e., $E_{a_1 a_2}$, the zero-field energy of equ. (10) is large. This situation, in turn, permits the surprising result that external circularly polarized light of the appropriate frequency (the Larmor precession frequency) is able to excite a resonance coupling resulting in large internal magnetic moment enhancement, the d-d metal transition involved being magnetic dipole and quadrupole-allowed, but electric dipole-forbidden.

VI. REFERENCES

1. Barrett, T.W., 1981, Chem. Phys. Lett. 78, 125.
2. Barrett, T.W., 1982, J. Chem Soc. Chem. Comm. 789, 9.
3. Chiu, Y-N., 1970, J. Chem. Phys. 52, 3641.
4. Tanabe, Y. and Sugano, S., 1954, J. Phys. Soc. Japan 9, 766.
5. Sonnich Mortensen, O. and Konigstein, J.S., 1968, J. Chem. Phys. 48, 3971.
6. Child, M.S. and Longuet-Higgins, H.C., 1961, Phil. Trans. Roy. Soc. A254, 259.
7. McClain, W.M., 1971, J. Chem. Phys. 55, 2789.
8. Plazcek, G., 1934, in Rayleigh and Raman Scattering, UCRL Trans. No. 526L from Handbuch der Radiologie (ed. by E. Marx), Leipzig, Akademische Verlagsgesellschaft VI, 2, 209.
9. Pézolet, M., Nafie, L.A., and Peticolas, W.L., 1973, J. Raman Spectroscopy 1, 455.
10. Nestor, J. and Spiro, T.G., 1973, J. Raman Spectroscopy 1, 539.
11. Spiro, T.G. and Strekas, T.C., 1972, Proc. Nat. Acad. Sci. 69, 2622.
12. Hamaguchi, H., Harada, I. and Schimanouchi, T., 1975, Chem. Phys. Lett. 32, 103.
13. Stein, P., Brown, J.M., and Spiro, T.G., 1977, Chem. Phys. 25, 237.
14. Hamaguchi, H. and Schimanouchi, T., 1976, Chem. Phys. Lett. 38, 370.
15. Clark, R.H.H. and Turtle, P.C., 1976, J. Chem. Soc. Faraday II 72, 1885.
16. Sonnich Mortensen, O. and Hassing, S., 1980, pp. 1-60 in Advances in Infrared and Raman Spectroscopy, Vol. 6, R.T.H. Clark and R.E. Hester (eds), Heyden, London.
17. Shriver, D.F. and Dunn, J.B.R., 1974, Appl. Spectr. 28, 319.
18. Kiefer, W., 1977, pp. 1-41 in R.J.H. Clark and R.E. Hester (eds) Advances in Infrared and Raman Spectroscopy, Vol. 3, Heyden, London.

19. Monson, P.R. and McClain, W.M., 1970, J. Chem. Phys. 53, 29.

20. Monson, P.R. and McClain, W.M., 1972, J. Chem. Phys. 56, 4817.

21. McClain, W.M., 1972, J. Chem Phys. 57, 2264.

22. Barron, L.D., 1978, Chap. 6 pp. 271-331 in R.J.H. Clark and R.E. Hester (eds) Advances in Infrared and Raman Spectroscopy, Vol. 4, Heyden, London.

23. Barron, L.D., 1982, Molecular Light Scattering and Optical Activity, Cambridge University Press.

24. Fiutak, J., 1963, Can. J. Phys. 41, 12.

25. Göppert-Mayer, M., 1931, Ann. Physik 9, 273.

26. Herzfeldt, K.F. and Goppert-Mayer, M., 1936, Phys. Rev. 49, 332.

27. Buckingham, A.D., 1967, Adv. Chem. Phys. 12, 107.

28. Barron, L.D. and Buckingham, A.D., 1975, Ann. Rev. Phys. Chem. 26, 381.

29. Barron, L.D., 1977, J. Chem. Soc. London Perkin Trans. II, 1074.

30. Barron, L.D., 1977, J. Chem. Soc. London Perkin Trans. II, 1790.

31. Spiro, T.G. and Stein, P., 1977, Ann. Rev. Phys. Chem. 28, 501.

32. Adar, F., pp. 167-209 in D. Dolphin (ed) The Porphyrins, Physical Chemistry, Part A, Academic, 1978.

33. Schooley, D.A., Bunnenberg, E. and Djerassi, C., 1965, Proc. Nat. Acad. Sci. 53, 579.

34. Melki, G., 1972, Biochim. Biophys. Acta 263, 226.

35. Yoshida, S., Iizuka, T., Nozawa, T. and Hatano, H., 1975, Biochim. Biophys. Acta 405, 122.

36. Hatano, M. and Nozawa, T., 1978, Adv. Biophys. 11, 95.

37. Sutherland, J.C., Vickery, L.W. and Klein, M.P., 1974, Rev. Sci. Instr. 45, 1089.

38. Treu, J.I. and Hopfield, J.J., 1975, J. Chem. Phys. 63, 613.

39. Cheng, J.C., Osborne, G.A., Stephens, P.J. and Eaton, W.A., 1973, Nature 241, 193.

40. Atkins, P.W. and Barron, L.D., 1968, Proc. Roy. Soc. A304, 303.

41. Atkins, P.W. and Barron, L.D., 1968, Proc. Roy. Soc. A306, 119.

42. Atkins, P.W. and Barron, L.D., 1969, Mol. Phys. 16, 453.

43. Atkins, P.W. and Miller, M.H., 1968, Mol. Phys. 15, 491.

44. Atkins, P.W. and Miller, M.H., 1968, Mol. Phys. 15, 503.

45. Atkins, P.W. and Wooley, R.G., 1970, Proc. Roy. Soc. London A319, 549.

46. Wooley, R.G., 1971, Proc. Roy. Soc. London A321, 557.

47. Barron, L.D., 1976, pp. 96-124 in Molecular Spectroscopy, Vol. 4, R.F. Barrow, D.A. Long and J. Sheriden (eds), The Chemical Society, London.

48. Barron, L.D. and Buckingham, A.D., 1971, Mol. Phys. 20, 1111.

49. Pershan, P.S., Van der Ziel, J.P. and Malmstrom, K.D., 1966, Phys. Rev. 143, 574.

50. Pershan, P.S., 1963, Phys. Rev. 130, 919.

51. Wallace, R., 1966, Mol. Phys. 11, 457.

52. Sutherland, J.C. and Klein, M.P., 1972, J. Chem. Phys. 57, 76.

53. Sutherland, J.C., Axelrod, D. and Klein, M.P., 1971, J. Chem. Phys. 54, 2888.

54. Barth, G., Linder, R.E., Bunnenberg, E., Djerassi, C., Seamans, L. and Moscowitz, A., 1974, J. Chem. Soc. Perkin II, 696.

55. Larmor, J., 1897, Phil. Mag. 44, 503.

56. Larmor, J., 1899, Proc. Cambr. Phil. Soc. 10, 181.

57. Larmor, J., 1900, Aether and Matter, Cambridge Univ. Press.

58. Barrett, T.W., 1979, J. Raman Spec. 8, 122.

59. Bromberg, P.A. and Jensen, W.M., 1967, J. Lab. Clin. Med. 70, 480.

60. Allen, D.W. and Wyman, J., 1954, Rev. Hematol. 9, 155.

61. Bunn, H.F., 1972, in Hemoglobin and Red Cell Structure and Function, G. Brewer (ed), Plenum, NY.

62. Rossi-Bernardi, L., Luzanna, M. and Samaja, M., 1975, FEBS Lett. 59, 15.

63. May, A. and Huehns, E.R., 1972, Br. J. Hematol. 22, 599.

64. Spiro, T.G. and Loehr, T.M., 1975, pp. 98-142 in Advances in Infrared and Raman Spectroscopy, Vol. 1, R.J.H. Clark and R.E. Hester (eds), Heyden, London.

65. Spiro, T.G. and Strekas, T.C., 1974, J. Am. Chem. Soc. 96, 338.

66. Hochstrasser, R.M. and Nyi, C.A., 1979, J. Chem. Phys. 70, 1112.

67. Kitagawa, T., Abe, M., Kyogoku, Y., Ogoshi, H., Watanabe, E. and Yoshida, Z., 1976, J. Phys. Chem. 80, 1181.

68. Kitagawa, T., Kyogoku, Y., Iizuka, T., Saito, M.I. and Yamanaka, T., 1975, J. Biochem. 78, 719.

69. Wilson, E.B., Decius, J.C. and Cross, P.C., 1955, Molecular Vibrations, McGraw-Hill, NY.

70. Tang, J. and Albrecht, A.C., 1970, pp. 33-67 in Raman Spectroscopy, Vol. 2, H.A. Szymanski (ed), Plenum, NY.

71. Shelnutt, J.A., Rousseau, D.L., Friedman, J.M. and Simon, S.R., 1979, Proc. Nat. Acad. Sci. U.S.A. 76, 4409.

72. Spiro, T.C. and Burke, J.M., 1976, J. Am. Chem. Soc. 98, 5482.

73. Bleaney, B. and Stevens, K.W.H., 1953, Reports on Progress in Physics 16, 108.

74. Bowers, K.D. and Owen, J., 1955, Reports on Progress in Physics 18, 304.

75. Orton, J.W., 1959, Reports on Progress in Physics 22, 204.

76. Ballhausen, C.J., 1962, Introduction to Ligand Field Theory, McGraw-Hill, New York.

77. Zerner, M. and Gouterman, M., 1966, Theor. Chim. Acta 4, 44.

78. Kitagawa, T., Abe, M., Kyogoku, Y., Ogoshi, H., Sugimoto, H. and Yoshida, Z., 1977, Chem. Phys. Lett. 48, 55.

79. Buchler, J.W., Kokish, W. and Smith, P.D., 1978, Structure and Bonding 34, 79.

80. Gouterman, M., 1959, J. Chem. Phys. 30, 1139.

81. Gouterman, M., 1961, J. Mol. Spectroscopy 6, 138.

82. Day, P., Scregg, G. and Williams, R.J.P., 1964, Biopolymers Symp. No. 1, 271.

83. Smith, D.W. and Williams, R.J.P., 1968, Biochem. J. 110, 297.

84. Smith, D.W. and Williams, R.J.P., 1970, Structure and Bonding 7, 1.

85. Zerner, M., Gouterman, M. and Kobayaski, H., 1966, Theor. Chim. Acta 6, 363.

86. Gouterman, M., Yamanshi, B.S. and Kwiram, A.L., 1972, J. Chem. Phys. 56, 4073.

87. Gouterman, M., 1973, Ann. N.Y. Acad. Sci. 206, 70.

This Page Intentionally Left Blank

END

FILMED

11-85

DTIC